BJR

https://doi.org/10.1259/bjr.20180886

Received: 15 October 2018 | Revised: 05 April 2019 | Accepted: 12 April 2019

Cite this article as:
Rubbert C, Mathys C, Jockwitz C, Hartmann CJ, Eickhoff SB, Hoffstaedter F, et al. Machine-learning identifies Parkinson's disease patients based on resting-state between-network functional connectivity. *Br J Radiol* 2019; **92**: 20180886.

ADVANCES IN NEURODEGENERATIVE AND PSYCHIATRIC IMAGING SPECIAL FEATURE: FULL PAPER

Machine-learning identifies Parkinson's disease patients based on resting-state between-network functional connectivity

[1]CHRISTIAN RUBBERT, MD, [1,2]CHRISTIAN MATHYS, MD, [3,4]CHRISTIANE JOCKWITZ, PhD, [5,6]CHRISTIAN J HARTMANN, MD, [7,8]SIMON B EICKHOFF, MD, [7,8]FELIX HOFFSTAEDTER, PhD, [3,9,10]SVENJA CASPERS, MD, [5,8]CLAUDIA R EICKHOFF, MD, [1]BENJAMIN SIGL, MD, [1]NIKOLAS A TEICHERT, MD, [11]MARTIN SÜDMEYER, MD, [1]BERND TUROWSKI, MD, [5,6]ALFONS SCHNITZLER, MD and [1]JULIAN CASPERS, MD

[1]University Dusseldorf, Medical Faculty, Department of Diagnostic and Interventional Radiology, D-40225 Dusseldorf, Germany
[2]Institute of Radiology and Neuroradiology, Evangelisches Krankenhaus, University of Oldenburg, Germany
[3]Institute of Neuroscience and Medicine (INM-1) Research Centre Jülich, Jülich, Germany
[4]Department of Psychiatry, Psychotherapy and Psychosomatics, RWTH Aachen University, Medical Faculty, Aachen, Germany
[5]Institute of Clinical Neuroscience and Medical Psychology Medical Faculty Heinrich-Heine-University, Düsseldorf, Germany
[6]Department of Neurology, Center for Movement Disorders and Neuromodulation, Medical Faculty, Heinrich Heine University, Düsseldorf, Germany
[7]Institute for Systems Neuroscience, Medical Faculty, Heinrich-Heine University, Dusseldorf, Germany
[8]Institute of Neuroscience and Medicine (INM-7), Research Centre Jülich, Germany
[9]JARA-BRAIN Jülich-Aachen Research Alliance, Jülich, Germany
[10]Institute for Anatomy I, University Dusseldorf, Medical Faculty, Düsseldorf, Germany
[11]Department of Neurology, Ernst-von-Bergmann Klinikum, Potsdam, Germany

Address correspondence to: Dr Christian Rubbert
E-mail: *christian.rubbert@med.uni-duesseldorf.de*

Objective: Evaluation of a data-driven, model-based classification approach to discriminate idiopathic Parkinson's disease (PD) patients from healthy controls (HC) based on between-network connectivity in whole-brain resting-state functional MRI (rs-fMRI).

Methods: Whole-brain rs-fMRI (EPI, TR = 2.2 s, TE = 30 ms, flip angle = 90°. resolution = 3.1 × 3.1 × 3.1 mm, acquisition time ≈ 11 min) was assessed in 42 PD patients (medical OFF) and 47 HC matched for age and gender. Between-network connectivity based on full and L2-regularized partial correlation measures were computed for each subject based on canonical functional network architectures of two cohorts at different levels of granularity (Human Connectome Project: 15/25/50/100/200 networks; 1000BRAINS: 15/25/50/70 networks). A Boosted Logistic Regression model was trained on the correlation matrices using a nested cross-validation (CV) with 10 outer and 10 inner folds for an unbiased performance estimate, treating the canonical functional network architecture and the type of correlation as hyperparameters. The number of boosting iterations was fixed at 100. The model with the highest mean accuracy over the inner folds was trained using an non-nested 10-fold 20-repeats CV over the whole dataset to determine feature importance.

Results: Over the outer folds the mean accuracy was found to be 76.2% (median 77.8%, SD 18.2, IQR 69.4 – 87.1%). Mean sensitivity was 81% (median 80%, SD 21.1, IQR 75 – 100%) and mean specificity was 72.7% (median 75%, SD 20.4, IQR 66.7 – 80%). The 1000BRAINS 50-network-parcellation, using full correlations, performed best over the inner folds. The top features predominantly included sensorimotor as well as sensory networks.

Conclusion: A rs-fMRI whole-brain-connectivity, data-driven, model-based approach to discriminate PD patients from healthy controls shows a very good accuracy and a high sensitivity. Given the high sensitivity of the approach, it may be of use in a screening setting.

Advances in knowledge: Resting-state functional MRI could prove to be a valuable, non-invasive neuroimaging biomarker for neurodegenerative diseases. The current model-based, data-driven approach on whole-brain between-network connectivity to discriminate Parkinson's disease patients from healthy controls shows promising results with a very good accuracy and a very high sensitivity.

INTRODUCTION

Parkinson's disease (PD) is the second most common neurodegenerative disorder after Alzheimer's disease and is of growing relevance for public health in the ageing society. The diagnosis is primarily based on clinical history and neurological examinations. Progressive motor symptoms are the hallmark of the disease, with otherwise unexplainable bradykinesia, muscular rigidity, rest tremor or postural instability as the main symptoms. Non-motor symptoms include sensory and autonomic dysfunction, disorders of mood and affect, as well as complex behavioural disorders. Especially depression or hyposmia may predate the clinically apparent onset of PD.[1]

The development of motor symptoms is primarily attributed to progressive loss of dopaminergic neurons in the substantia nigra, which results in a destabilization of the basal ganglia circuits. The pathogenesis behind non-motor symptoms is not fully understood.[1] Beyond the established basal ganglia pathways, structural and functional dysregulations in the cortico-subcortical networks, especially in the cortico-striatal and cortico-cortical connections have been observed.[2,3]

Even with established and well-tested diagnostic criteria published by the UK Parkinson's Disease Society Brain Bank in 1988,[4] clinical diagnosis of PD may be challenging in certain cases. Overall, 82.7% of PD diagnoses are accurate as confirmed by autopsy. The diagnostic accuracy of movement disorder experts was found to be 79.6% at the initial visit and improved to 83.9% after refinement of diagnosis on a follow-up examination. Non-experts were 73.8% accurate.[5] Therefore, a robust biomarker would be beneficial in the diagnosis of PD and could significantly enhance clinical evaluation in certain diagnostic dilemmas.

Resting-state functional MRI (rs-fMRI) has emerged in recent years as a valuable, non-invasive tool to study functional connectivity within or between functional networks. These resting state functional networks are derived from clustering concurrent and spontaneous fluctuations of blood-oxygenation-level-dependent (BOLD) signal in time-resolved MRI sequences in the absence of a specific task. Rs-fMRI has been widely used to study a number of neurodegenerative and neuropsychiatric diseases and to gain insights into the brain's organization.[6,7] In PD, resting-state functional connectivity has repeatedly been studied under varying hypotheses, usually examining aberrations in specific networks or areas, such as the basal ganglia,[8,9] sensorimotor areas,[8] or areas related to executive function.[9] For example, a negative functional correlation between the subthalamic nucleus and the primary motor cortex was predictive for a better treatment response in Deep Brain Stimulation (DBS) patients.[10]

Given the interplay of different symptoms, *e.g.* of motor and non-motor symptoms, and functional connectivity changes found between and across different functional networks, we hypothesize, that aberrations in the whole-brain connectivity in PD patients can be used as a non-invasive, neuroimaging-based biomarker. Essentially, this hypothesis is based on the emerging understanding of PD as a "disconnection syndrome".[11] Given the complexity of the problem, we applied a supervised machine learning (ML) technique, which can learn patterns from existing, complex, labelled data to generalise to previously unseen data. In the current study, we evaluated a data-driven, model-based, supervised classification approach to identify PD patients based on between-network functional connectivity in whole-brain resting-state fMRI.

METHODS AND MATERIALS

The study was approved by the local ethics committee and performed in accordance with the declaration of Helsinki. All subjects provided written informed consent prior to study inclusion.

Sample

42 patients from the local department of neurology, diagnosed with idiopathic PD, and 47 healthy controls (HC), without any record of neurological or psychiatric disorders, were included in the current analysis (Table 1). Patients and subjects were included from a pre-existing PD/HC pool[9,12] by determining

Table 1. Characteristics of the Parkinson's disease and healthy controls sample. * MDRS was available in 41 of 42 patients

	Healthy controls	Parkinson's disease patients
n	47	42
Age (years): mean ± SD	60.2 ± 8.9	61.8 ± 9.6
Sex: female/male	22 (47%) / 25 (53%)	15 (36%) / 27 (64%)
Disease duration (years): mean ± SD		9.7 ± 5.5
Modified Hoehn & Yahr stage: median (IQR)		2.75 (2-3)
UPDRS-III (OFF): median (IQR)		34 (26–38.8)
UPDRS-III (ON): median (IQR)		16.5 (12.2–25)
Levodopa Equicalent Dose (LED): mean ± SD		1062.8 ± 364.2
Mattis Dementia Rating Scale (MDRS)*: median (IQR)		140 (137–142)
Symptom lateralization: right/left		16 (38.1%) / 26 (61.9%)
Motor type: akinetic rigid/tremor dominant/mixed type		14 (33.3%) / 6 (14.3%) / 22 (52.4%)

the largest sample where age and gender did not differ significantly between the PD and HC subjects (two-sample t-tests for age, χ^2-test for gender, all $p > 0.1$). Patients with non-idiopathic Parkinson syndromes, severe dementia, major depression and ineligibility for MRI had not been included in the pool.

Diagnosis of idiopathic PD was based on the aforementioned criteria by a board-certified neurologist.[4] All patients were under long-term dopaminergic treatment with individual drug regimens optimized for their individual needs, including levodopa, catechol-O-methyltransferase inhibitors, dopamine agonists and further symptomatic drugs. Rs-fMRI scans were acquired after at least 12 h of withdrawal of the patient's regular dopaminergic medication (medical OFF).

rs-fMRI

Whole-brain rs-fMRI was acquired using an echo-planar imaging (EPI) sequence on a 3T MRI scanner (Siemens Trio, Erlangen, Germany) to obtain BOLD time series (time points = 300, TR = 2.2 s, TE = 30 ms, flip angle = 90°, field of view (FoV) = 200×200 mm axial plane, slices = 36, voxel size = 3.1 mm^3, acquisition time ≈ 11 min).

Furthermore, a T_1 weighted three-dimensional magnetization prepared rapid gradient-echo sequence (MPRAGE, TR = 2.3 s, TE = 2.96 ms, TI = 900 ms, flip angle = 8°, FoV = 240×256 mm sagittal plane, slices = 192, voxel size = 1 mm^3) was acquired for structural information and registration during pre-processing.

rs-fMRI pre-processing

Pre-processing and analysis of rs-fMRI was performed using the Oxford Centre for Functional MRI of the Brain (FMRIB) Software Library (FSL) v5.0.[13]

The first five images of the fMRI time-series were discarded to account for magnetic saturation effects. EPI volumes were motion-corrected. The six rigid-body parameter time series yielded from motion correction were used for later EPI signal denoising. Brain-extraction was performed on the motion-corrected EPI volumes and the structural MRIs with FMRIB's Brain Extraction Tool (BET2).[14] EPIs were spatially smoothed with a 5 mm full width at half maximum gaussian kernel and normalized for intensity variations over time. High-pass filtering with a 150 s cut-off was conducted. FMRIB's ICA-based Xnoisifier (FIX) was then used to automatically denoise the rs-fMRI data.[15,16] Finally, EPI volumes were linearly co-registered to their respective structural image, and subsequently spatially normalized by applying the deformations yielded from linear and non-linear registration of the structural image to the MNI152 standard reference space.

Between-network connectivity

Griffanti et al. suggests to use sets of healthy brains, independent of the sample under investigation, for analysis of disease-related network alterations.[17] Therefore, we relied on canonical functional network architecture from two large population-based samples, the Human Connectome Project (HCP) and 1000BRAINS.

HCP publicly released network definitions based on independent component analysis (ICA) on elaborately acquired and (pre-)processed data[18–20] at different levels of granularity (15, 25, 50, 100. 200 and 300 networks; July 2017 HCP1200 Parcellation + Timeseries+Netmats release: https://db.humanconnectome.org/data/projects/HCP_1200). Essentially, FMRIB's Multivariate Exploratory Linear Optimized Decomposition into Independent Components (MELODIC)'s[18,21] incremental group-level principal component analysis (Group-PCA) from 812 subjects ("recon2" subjects, aged 22 to 35, with nine subjects noted as 36+) was fed into MELODIC's group-level ICA (Group-ICA) applying spatial-ICA to generate the network definitions (extensive documentation available at https://www.humanconnectome.org/storage/app/media/documentation/s1200/HCP1200-DenseConnectome+PTN+Appendix-July2017.pdf). Due to computational restraints the 300 network parcellation was excluded from the current study, while all other parcellations were used.

1000BRAINS is a population-based sample investigating the inter-individual variability of brain structure and function during aging.[7] The acquisition, also on a Siemens Trio 3T, and the pre-processing protocol, was identical to the current study, except for the high-pass filtering at 100 ms (current study: 150 ms).[7,19] Functional network definitions based on group-ICA at a granularity of 15, 25, 50, and 70 components were derived from the 1000BRAINS sample using MELODIC in 267 healthy older adults in the same age range as the PD/HC group (mean age 61.9 years; SD 8.8; 157 males).

The network maps from HCP and 1000BRAINS were used as spatial regressors on the fully pre-processed EPIs of the current study to extract subject-specific timeseries for each network using the first step of FSL's Dual Regression.[20] Resulting time-series were variance-normalized.

For each set of networks, between-network connectivity was calculated using FSLNets v0.6.3 (https://fsl.fmrib.ox.ac.uk/fsl/fslwiki/FSLNets) in GNU Octave v4.0.3 (https://www.gnu.org/software/octave/). Pearson correlations ("full correlations") and L2-norm Ridge Regression ($\rho = 0.01$, "partial correlations") between the network-specific time-series were calculated for each subject and transformed into Fisher's z-scores.

Modelling

Further analysis was performed using R v3.5.1 with the caret v6.0–81, rsample v0.0.4, and caTools v1.17.1.1 packages (https://cran.r-project.org/).

The upper triangle of the full and partial between-network correlation matrices of each subject and level of granularity were used for the model. Using only the upper triangle, without the diagonal, eliminates duplicate and non-informative features.

A boosted logistic regression model was trained on each of the correlation matrices to discriminate PD patients from HC. Essentially, boosting describes a combination of weak classifiers. In every iteration, a new „rule of thumb", just slightly better than average, will be determined by means of an additive logistic

Table 2. Individual results of each outer fold during nested cross-validation

Outer fold	Canonical network architecture	Type of correlation	Mean accuracy
1	HCP 25	Partial	33.3%
2	HCP 25	Full	85.7%
3	1000BRAINS 25	Full	88.9%
4	1000BRAINS 70	Full	66.7%
5	1000BRAINS 50	Full	77.8%
6	1000BRAINS 50	Full	77.8%
7	1000BRAINS 70	Full	100%
8	1000BRAINS 50	Full	77.8%
9	1000BRAINS 50	Full	66.7%
10	HCP 25	Full	87.5%

regression model. A nested cross-validation approach with 10 outer and 10 inner folds was chosen to find an unbiased estimate of the model performance.[22] The choice of canonical network architecture (1000BRAINS or HCP) and type of correlation (full or partial) were treated as hyperparameters to be tuned in the inner folds. The number of boosting iterations was fixed at 100. After selecting the best model with the highest mean accuracy over the inner folds, accuracy, sensitivity and specificity was calculated for the respective outer fold.

The hyperparameters yielding the mean best performance over the inner folds were used to determine feature importance by fitting a model in a non-nested, stratified, 20-repeats, 10-fold cross-validation over the whole dataset. Since no model-specific metric for feature importance exists, the importance of each feature is individually evaluated in a "filter" approach by means of a ROC-curve analysis and application of a series of cut-offs. The area under the curve is used as a measure of feature importance.[23] Since there is no model-specific metric, the feature importance was scaled from 0 to 1 and the features with a resulting scaled importance >0.8 were evaluated more closely. Furthermore, in that model, the patients misclassified in more than half of the repeats were explored to gain an insight into the classification process.

RESULTS

Evaluation was performed for each of the canonical network definitions from both samples (HCP: 15, 25, 50, 100 and 200; 1000BRAINS: 15, 25, 50 and 70) and for both types of correlation, fixed at 100 boosting iterations. After nested cross-validation the mean accuracy was found to be 76.2% (median 77.8%, SD 18.2, IQR 69.4–87.1%) over the outer folds. Mean sensitivity was 81% (median 80%, SD 21.1, IQR 75–100%) and mean specificity was 72.7% (median 75%, SD 20.4, IQR 66.7–80%). Table 2 shows the individual results of the outer folds.

The model yielding the highest mean accuracy over the inner folds during nested cross-validation was found to be the 1000BRAINS 50-network parcellation in the full correlations approach. As an example of model performances in the inner folds, the aggregated accuracies are shown in Figure 1. Classification on partial correlations showed an overall weaker performance over the inner folds. Here, the HCP 25-network-parcellation performed best, which was also the best performing parcellation for full correlations within the HCP sample.

Figure 1. Exemplary aggregated accuracies over the inner folds during the nested cross-validation for each canonical network architecture and type of correlation at 100 boosting iterations shown as a Box-Whisker-Plot.

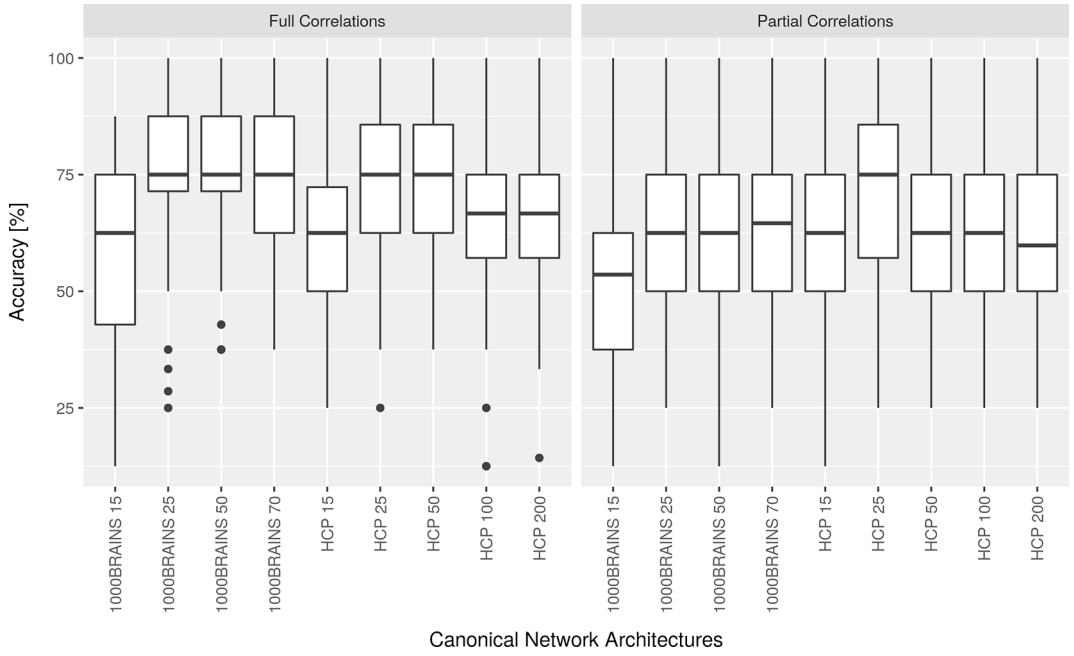

Figure 2. The top four features of the optimal model with a scaled feature importance >0.8.

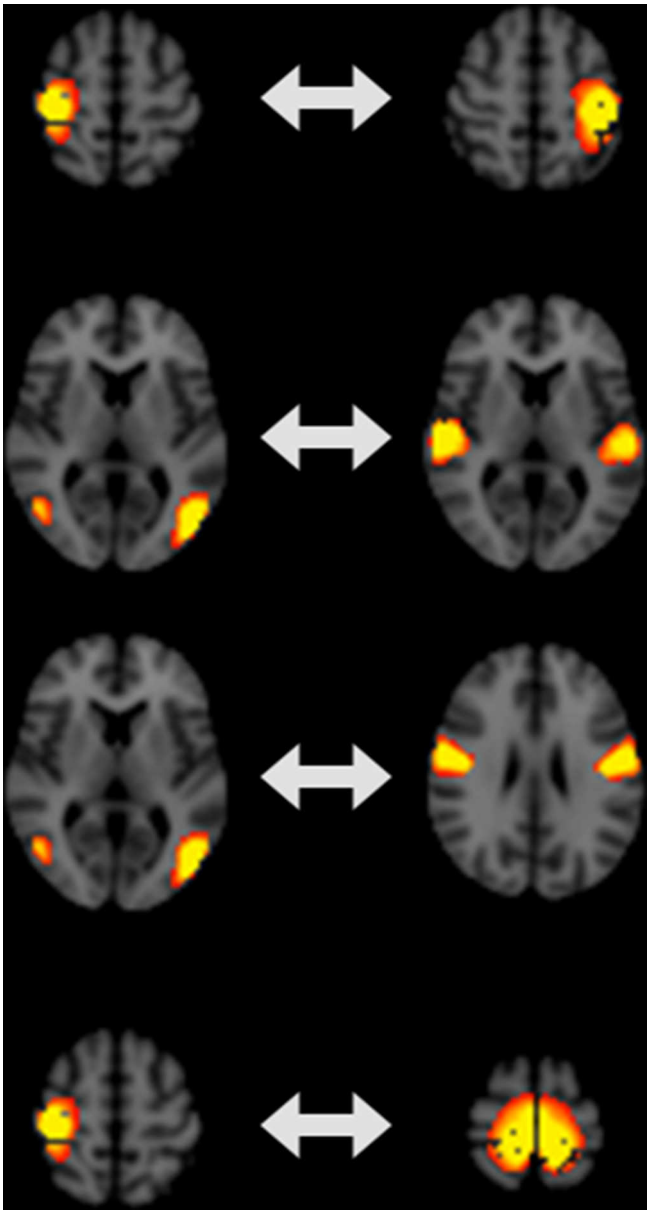

In the non-nested cross-validation approach, mean accuracy was 80.3% (median 80.9%, SD 3.7, IQR 77.8–82.1%). Mean sensitivity was 84.5% (median 84.5%, SD 4.3, IQR 81.9–87.9%) and mean specificity was 75.7% (median 76.3%, SD 5.7, IQR 72.1–80%). In analysis of feature importance, four features were found to have a scaled feature importance greater than 0.8 (Figure 2). The most important inter-network connection was found to be between a right lateralized and a left lateralized subpart of the sensorimotor network (SMN), each comprising the (pre-)supplementary motor area ((pre)SMA), ipsilateral primary sensorimotor cortex (SMC), thalamus and cerebellum. The second most important connection was found between a dorsal visual network comprising the parietooccipital cortex bilaterally and the auditory network, located at the superior temporal lobe and posterior insula bilaterally, and additionally included the cingulate cortex. This was followed by a correlation of the same dorsal visual network with the inferior part of the SMN, which comprised the primary motor and sensory cortex, posterior insula, thalamus, midbrain, and cerebellar areas bilaterally. The fourth most important correlation was between the aforementioned right lateralized SMN and a bihemispheric primary motor/premotor network located dorsally close to the midline.

In the exploration of 9 repeatedly misclassified patients, it was noted, that 6 (66.6%) had a right-lateralized onset of symptoms, whereas only 38.1% of PD patients in the whole sample were right-lateralized regarding motor symptoms.

DISCUSSION

This study aimed to evaluate a predictive model to discriminate PD from HC on the basis of between-network connectivity in whole-brain rs-fMRI. Our results show a very good accuracy and a very high sensitivity.

The ML model evaluated in this study is based on between-network connectivity, which has been investigated in a number of studies in PD.[24–26] For example, Gratton et al found that, using a graph-theoretical approach, alterations in between-network connectivity are more pronounced in PD than compared to within-network connectivity.[27] Our results, showing very good accuracy in predicting PD based on between-network connectivity, are in line with these studies, and are further backing the concept of PD as a "disconnection syndrome".[11]

There are a number of studies applying ML to identify PD, each with reasonable success. For example, an elaborate ensemble model trained on recorded speech samples was used to detect PD.[28] Furthermore, ML based on structural MR images was used to discriminate PD from progressive supranuclear palsy (PSP),[29] and an approach based on resting-state functional connectivity was used to separate PD patients with and without mild cognitive impairment.[30] In addition, whole-brain functional connectivity analyses have been conducted to gain further insights into the disease.[31–33] Other studies have proposed using functional connectivity of single networks as a neuroimaging biomarker, for example of the Basal Ganglia Network (BGN).[8,21] However, so far, no study has evaluated rs-fMRI based whole-brain between-network connectivity as a neuroimaging-based biomarker to diagnose PD.

The best-performing model in the inner folds during nested cross-validation was based on 50 networks derived from the 1000BRAINS cohort, which showed comparable results over inner folds and the unbiased performance expectations as determined by the outer folds. The model trained using a non-nested cross-validation approach on the whole dataset showed slightly higher performance measurements, which were overall in line with the performance estimates as determined by the nested cross-validation.

The analyses with 15 networks did not perform as well, most likely due to the network definitions being too coarse with

multiple intrinsic connectivity networks being merged into one component. Higher granularity (≥100) networks exhibited worse performance, likely due to the increasing fragmentation of intrinsic connectivity networks into sub networks. For example, consistent networks like the Default Mode Network (DMN) will be split into multiple components, which might lack a biological correlate at higher dimensionality. In this regard, our study might potentially indicate, that about 25–70 networks best reflect the actual, neurobiologically meaningful granularity of intrinsic connectivity networks and are a reasonable number to conduct network-based functional connectivity analyses.

Partial correlations showed a weaker performance compared to full correlations. Partial correlations provide more specific information about the direct connection between two networks by correcting for the influence of all other networks, as a strong (full) correlation between two networks could arise from the strong correlation of each network to a third network. However, the content of information about the subjects' entire connectivity is lowered by the mathematical procedure of regularization in each pair of networks. This reduced or less general information about connectivity within each feature for partial correlations might be the reason why full correlations performed better in our model-based classification than partial correlations.

Within the partial correlations, the 25-network-model from HCP performed best, which also performed best in full correlations across the HCP models. The reason, why the best performing HCP model comprised 25 components, while for 1000BRAINS the 50-network-model performed best, might possibly be found in data acquisition and processing. By means of specialized HCP-MR-scanners and sophisticated artefact-removal approaches, clean fMRI data of higher spatial and timing resolution is provided. For example, network definitions are based on a surface-based approach,[34] rather than volume-based processing as used in 1000BRAINS and our sample. Cleaner data of higher resolution could mean, that a smaller number of potentially more meaningful components are sufficient for discrimination. At this point in time, the number of actual networks in the brain still remains elusive and a higher dimensionality bears the risk of introducing artificial networks by segmenting actual networks.

The 1000BRAINS acquisition and pre-processing protocol is almost identical to the current study and included subjects of a similar age range. HCP acquired healthy young adults aged 22–35 years,[6] while 1000BRAINS included participants aged 55–85 years.[7] Age-related reorganization of functional networks has been demonstrated in the 1000BRAINS sample,[19] and for example age-related functional connectivity reductions in the DMN and occipital visual networks have been shown.[35] Both the similar acquisition and pre-processing workflow, as well as the similarly aged sample could explain the better performance of the 1000BRAINS sample in comparison to HCP.

It has to be noted, that the performance results of the non-nested cross-validation approach, which was used to determine feature importance, are probably too optimistic, since the selection of optimal hyperparameters was based on the entire dataset. However, the analysis of feature importance of the best performing model does allow for insights into the model. The SMN, which is separated into multiple subnetworks in the 1000BRAINS 50-network parcellation, played a crucial role in the features most important to the model. This is in line with a number of studies, which have repeatedly shown alterations in sensorimotor areas in patients with PD, for example aberrations in the primary motor cortex and SMA during finger movement or decreased functional connectivity within motor areas.[8,35–37] Using a graph-theory based resting-state fMRI analysis, Gratton et al. found, that, among all tested networks, the SMN showed the greatest alterations between PD patients and controls.[27] In this regard, the importance of the SMN in the network pathology of PD is further underlined by the feature importance of our classification approach. The second and third most important network pair contained the dorsal visual network. Interestingly, the auditory network was the counterpart in the second most important pair, which has only been sparsely reported on in PD.[36] However, disintegration between these two sensory areas as well as between the dorsal visual and sensorimotor networks may hint to impaired sensory integration for motor function, which is commonly observed in PD.[37] Especially network alterations in the dorsal visual (where) stream,[38] which processes spatial visual information for sensorimotor integration,[39] might be associated with impaired visuo-spatial integration for motor function in PD, and may thus contribute to the importance of the third most important network pair, *i.e.* the dorsal visual network and inferior part of the SMN.[37,40] The more frequent appearance of the right subpart of the SMN in the most important features might also relate to the overall better classification performance of patients showing left-lateralized motor symptoms, which were slightly overrepresented in our sample.

One of the limitations of the current study is the small number of included patients, although larger samples are rarely available in rs-fMRI analyses of PD. Patient's diagnosis of PD in the current study is based on clinical diagnosis and autopsy-proven confirmation was not available. As noted, clinical diagnosis in a follow-up visit to a movement disorder expert is only 83.9% accurate.[5] However, patients included in the current study had been seen multiple times by local movement disorder experts and, due to the mean disease duration of 9.7 years, atypical forms of Parkinsonism should be likely ruled out in the majority of cases. However, ground-truth in our study is still based on clinical diagnosis, which could have impacted the accuracy of the model. Future prospective studies, where diagnosis of PD is clinically reconsidered in case of misclassification by a classification model, as well as data samples substantiated by autopsy-proven diagnoses would be beneficial to further evaluate the use of machine-learning approaches in the evaluation of neurodegenerative disorders. Furthermore, the patients had been under dopaminergic medication for an extended period of time and were imaged in an induced medical OFF phase. Hence, it cannot be ruled out that some effects of the long-term dopaminergic medication might have influenced the changes observed between both subject groups, *e.g.* by reorganization of functional networks.[41] However, 12h of withdrawal reliably induce a Levodopa-deprived state since the plasma half-life of Levodopa is 1–3 h.

One of the main hurdles in widely deploying a model-based approach, as the one presented in the current study, is the very high heterogeneity in disease, rs-fMRI acquisition and pre-processing. For example, Badea et al. showed that global changes of functional connectivity are non-reproducible across three different datasets, while only some functional connectivity changes between "individual brain region pairs" were marginally consistent.[42] Uniform rs-fMRI acquisition and pre-processing are therefore mandatory. With the current approach, and network definitions based on an almost identical data acquisition and pre-processing, we achieved accuracies similar to those of clinical experts and outperformed non-experts,[5] although it has to be noted, that confirmation of diagnosis by autopsy would be desirable future studies. In this regard, the very good performance of our model is particularly remarkable regarding the quite heterogeneous PD sample included in the current study, which comprises patients from all stages of the disease, a wide range of disease duration and motor symptom severity as well as all motor subtypes. This should make our classification results generalizable and robust. However, larger, multi center, heterogeneous patient samples are needed to build even more robust models, which are then applicable to smaller, local patient collectives.

There are some studies investigating classification of PD based on structural T_1 weighted imaging. For example, Chen et al. applied different approaches to detect different diseases, yielding an accuracy of 68–80% for PD.[43] The previously mentioned study of Salvatore et al. applied a support vector machine model based on structural T_1 weighted images to differentiate PD, PSP, and HC, yielding an accuracy of more than 90%.[29] A straight-forward comparison of these results and the current study is not suitable, since the methodologies strongly varied and there are no structural metrics, which could capture inter-network connectivity. Furthermore, classification approaches of theses previous studies are not as conservative as in the current study and reported results could be too optimistic in regard to a general population. However, future studies should explore multi modality approaches by combining functional and structural neuroimaging information in a comparative way, such as the addition of diffusion tensor imaging (DTI) or a voxel-based morphometry (VBM) approach. Such approaches have for example been successfully applied to Alzheimer's disease patients,[44,45] but have so far not been widely studied in a predictive classification setting in Parkinson's disease.

Given the high sensitivity, a model-based approach could be useful in a screening setting. For example, it could be used in individuals with only mild symptoms of a movement disorder to decide if, how, and when to refer or follow up. Also, a larger, more diverse and carefully labelled sample of patients with a movement disorder could potentially allow to not only screen for those disorders, but also maybe differentiate idiopathic PD and atypical parkinsonian syndromes, such as multi system atrophy or PSP.

CONCLUSION

A model-based, data-driven approach to discriminate PD patients from healthy controls is feasible and shows a very good accuracy and a high sensitivity. 50 independent network components from 1000BRAINS's canonical functional network architecture performed best when analysing whole-brain functional connectivity with a full correlation approach. Given the high sensitivity, a model-based approach may be of use in a screening setting when trained on a larger sample.

ACKNOWLEDGMENTS

Data were provided in part by the Human Connectome Project, WU-Minn Consortium (Principal Investigators: David Van Essen and Kamil Ugurbil; 1U54MH091657) funded by the 16 NIH Institutes and Centers that support the NIH Blueprint for Neuroscience Research; and by the McDonnell Center for Systems Neuroscience at Washington University.

REFERENCES

1. Poewe W. Non-motor symptoms in Parkinson's disease. *Eur J Neurol* 2008; **15**(Suppl 1(s1)): 14–20. doi: https://doi.org/10.1111/j.1468-1331.2008.02056.x
2. Jellinger KA. Neuropathology of sporadic Parkinson's disease: evaluation and changes of concepts. *Mov Disord* 2012; **27**: 8–30. doi: https://doi.org/10.1002/mds.23795
3. Bartels AL, Leenders KL. Parkinson's disease: the syndrome, the pathogenesis and pathophysiology. *Cortex* 2009; **45**: 915–21. doi: https://doi.org/10.1016/j.cortex.2008.11.010
4. Gibb WR, Lees AJ. The relevance of the Lewy body to the pathogenesis of idiopathic Parkinson's disease. *Journal of Neurology, Neurosurgery & Psychiatry* 1988; **51**: 745–52. doi: https://doi.org/10.1136/jnnp.51.6.745
5. Rizzo G, Copetti M, Arcuti S, Martino D, Fontana A, Logroscino G. Accuracy of clinical diagnosis of Parkinson disease: a systematic review and meta-analysis. *Neurology* 2016; **86**: 566–76. doi: https://doi.org/10.1212/WNL.0000000000002350
6. Van Essen DC, Smith SM, Barch DM, Behrens TEJ, Yacoub E, Ugurbil K, et al. The WU-Minn human connectome project: an overview. *Neuroimage* 2013; **80**: 62–79. doi: https://doi.org/10.1016/j.neuroimage.2013.05.041
7. Caspers S, Moebus S, Lux S, Pundt N, Schütz H, Mühleisen TW, et al. Studying variability in human brain aging in a population-based German cohort-rationale and design of 1000BRAINS. *Front Aging Neurosci* 2014; **6**: 149. doi: https://doi.org/10.3389/fnagi.2014.00149
8. Tessitore A, Giordano A, De Micco R, Russo A, Tedeschi G. Sensorimotor connectivity in Parkinson's disease: the role of functional neuroimaging. *Front Neurol* 2014; **5**(10 Suppl 3): 180. doi: https://doi.org/10.3389/fneur.2014.00180
9. Caspers J, Mathys C, Hoffstaedter F, Südmeyer M, Cieslik EC, Rubbert C, et al. Differential functional connectivity alterations of two subdivisions within the right dlPFC in Parkinson's disease. *Front*

Hum Neurosci 2017; **11**: 288. doi: https://doi.org/10.3389/fnhum.2017.00288
10. Horn A, Reich M, Vorwerk J, Li N, Wenzel G, Fang Q, et al. Connectivity predicts deep brain stimulation outcome in Parkinson disease. *Ann Neurol* 2017; **82**: 67–78. doi: https://doi.org/10.1002/ana.24974
11. Cronin-Golomb A. Parkinson's disease as a disconnection syndrome. *Neuropsychol Rev* 2010; **20**: 191–208. doi: https://doi.org/10.1007/s11065-010-9128-8
12. Mathys C, Caspers J, Langner R, Südmeyer M, Grefkes C, Reetz K, et al. Functional connectivity differences of the subthalamic nucleus related to Parkinson's disease. *Hum Brain Mapp* 2016; **37**: 1235–53.
13. Jenkinson M, Beckmann CF, Behrens TEJ, Woolrich MW, Smith SM. Fsl. *Neuroimage* 2012; **62**: 782–90. doi: https://doi.org/10.1016/j.neuroimage.2011.09.015
14. Smith SM. Fast robust automated brain extraction. *Hum Brain Mapp* 2002; **17**: 143–55. doi: https://doi.org/10.1002/hbm.10062
15. Salimi-Khorshidi G, Douaud G, Beckmann CF, Glasser MF, Griffanti L, Smith SM. Automatic denoising of functional MRI data: combining independent component analysis and hierarchical fusion of classifiers. *NeuroImage* 2014; **90**: 449–68. doi: https://doi.org/10.1016/j.neuroimage.2013.11.046
16. Griffanti L, Salimi-Khorshidi G, Beckmann CF, Auerbach EJ, Douaud G, Sexton CE, et al. ICA-based artefact removal and accelerated fMRI acquisition for improved resting state network imaging. *NeuroImage* 2014; **95**: 232–47. doi: https://doi.org/10.1016/j.neuroimage.2014.03.034
17. Griffanti L, Rolinski M, Szewczyk-Krolikowski K, Menke RA, Filippini N, Zamboni G, et al. Challenges in the reproducibility of clinical studies with resting state fMRI: an example in early Parkinson's disease. *NeuroImage* 2016; **124**((Pt A)): 704–13. doi: https://doi.org/10.1016/j.neuroimage.2015.09.021
18. Smith SM, Hyvärinen A, Varoquaux G, Miller KL, Beckmann CF. Group-PCA for very large fMRI datasets. *NeuroImage* 2014; **101**: 738–49. doi: https://doi.org/10.1016/j.neuroimage.2014.07.051
19. Jockwitz C, Caspers S, Lux S, Eickhoff SB, Jütten K, Lenzen S, et al. Influence of age and cognitive performance on resting-state brain networks of older adults in a population-based cohort. *Cortex* 2017; **89**: 28–44. doi: https://doi.org/10.1016/j.cortex.2017.01.008
20. Nickerson LD, Smith SM, Öngür D, Beckmann CF. Using dual regression to investigate network shape and amplitude in functional connectivity analyses. *Front. Neurosci.* 2017; **11**: 115. doi: https://doi.org/10.3389/fnins.2017.00115
21. Beckmann CF, Smith SM. Probabilistic independent component analysis for functional magnetic resonance imaging. *IEEE Trans. Med. Imaging* 2004; **23**: 137–52. doi: https://doi.org/10.1109/TMI.2003.822821
22. Cawley GC, Talbot NLC. On Over-fitting in model selection and subsequent selection bias in performance evaluation. *Journal of Machine Learning Research* 2010; **11**: 2079–107.
23. Kuhn M. Building Predictive Models in *R* Using the **caret** Package. *Journal of Statistical Software* 2008; **28**: 1–26. doi: https://doi.org/10.18637/jss.v028.i05
24. Baggio H-C, Sala-Llonch R, Segura B, Marti M-J, Valldeoriola F, Compta Y, et al. Functional brain networks and cognitive deficits in Parkinson's disease. *Human Brain Mapping* 2014; **35**: 4620–34. doi: https://doi.org/10.1002/hbm.22499
25. Onu M, Badea L, Roceanu A, Tivarus M, Bajenaru O. Increased connectivity between sensorimotor and attentional areas in Parkinson's disease. *Neuroradiology. Springer Berlin Heidelberg* 2015; **57**: 957–68.
26. Peraza LR, Nesbitt D, Lawson RA, Duncan GW, Yarnall AJ, Khoo TK, et al. Intra- and inter-network functional alterations in Parkinson's disease with mild cognitive impairment. *Hum. Brain Mapp.* 2017; **38**: 1702–15. doi: https://doi.org/10.1002/hbm.23499
27. Gratton C, Koller JM, Shannon W, Greene DJ, Maiti B, Snyder AZ, Petersen SE, et al. Emergent functional network effects in Parkinson disease. *Cereb Cortex* 2018; **5**(Suppl 17). doi: https://doi.org/10.1093/cercor/bhy121
28. Mandal I, Sairam N. New machine-learning algorithms for prediction of Parkinson's disease. International Journal of systems science. *Taylor & Francis* 2014; **45**: 647–66.
29. Salvatore C, Cerasa A, Castiglioni I, Gallivanone F, Augimeri A, Lopez M, et al. Machine learning on brain MRI data for differential diagnosis of Parkinson's disease and progressive supranuclear palsy. *Journal of Neuroscience Methods* 2014; **222**: 230–7. doi: https://doi.org/10.1016/j.jneumeth.2013.11.016
30. Abós A, Baggio HC, Segura B, García-Díaz AI, Compta Y, Martí MJ, et al. Discriminating cognitive status in Parkinson's disease through functional connectomics and machine learning. *Sci Rep* 2017; **7**: 45347. doi: https://doi.org/10.1038/srep45347
31. Pan P, Zhang Y, Liu Y, Zhang H, Guan D, Xu Y. Abnormalities of regional brain function in Parkinson's disease: a meta-analysis of resting state functional magnetic resonance imaging studies. *Sci Rep. Nature Publishing Group* 2017; **7**: 40469.
32. de Schipper LJ, Hafkemeijer A, van der Grond J, Marinus J, Henselmans JML, van Hilten JJ. Altered whole-brain and network-based functional connectivity in Parkinson's disease. *Front. Neurol.* 2018; **9**: 419. doi: https://doi.org/10.3389/fneur.2018.00419
33. Wang H, Chen H, Wu J, Tao L, Pang Y, Gu M, et al. Altered resting-state voxel-level whole-brain functional connectivity in depressed Parkinson's disease. *Parkinsonism & Related Disorders* 2018; **50**: 74–80. doi: https://doi.org/10.1016/j.parkreldis.2018.02.019
34. Glasser MF, Sotiropoulos SN, Wilson JA, Coalson TS, Fischl B, Andersson JL, et al. The minimal preprocessing pipelines for the human connectome project. *NeuroImage* 2013; **80**: 105–24. doi: https://doi.org/10.1016/j.neuroimage.2013.04.127
35. Mowinckel AM, Espeseth T, Westlye LT. Network-specific effects of age and in-scanner subject motion: a resting-state fMRI study of 238 healthy adults. *NeuroImage* 2012; **63**: 1364–73. doi: https://doi.org/10.1016/j.neuroimage.2012.08.004
36. Díez-Cirarda M, Strafella AP, Kim J, Peña J, Ojeda N, Cabrera-Zubizarreta A, et al. Dynamic functional connectivity in Parkinson's disease patients with mild cognitive impairment and normal cognition. *NeuroImage: Clinical* 2018; **17**: 847–55. doi: https://doi.org/10.1016/j.nicl.2017.12.013
37. Abbruzzese G, Berardelli A. Sensorimotor integration in movement disorders. *Mov Disord.* 2003; **18**: 231–40. doi: https://doi.org/10.1002/mds.10327
38. Mishkin M, Ungerleider LG, Macko KA. Object vision and spatial vision: two cortical pathways. *Trends in Neurosciences* 1983; **6**: 414–7. doi: https://doi.org/10.1016/0166-2236(83)90190-X
39. Culham JC, Kanwisher NG. Neuroimaging of cognitive functions in human parietal cortex. *Current Opinion in Neurobiology* 2001; **11**: 157–63. doi: https://doi.org/10.1016/S0959-4388(00)00191-4
40. Costa A, Peppe A, Dell'Agnello G, Carlesimo GA, Murri L, Bonuccelli U, et al.

Dopaminergic modulation of visual-spatial working memory in Parkinson's disease. dement Geriatr Cogn Disord. *Karger Publishers* 2003; **15**: 55–66.

41. Tahmasian M, Bettray LM, van Eimeren T, Drzezga A, Timmermann L, Eickhoff CR, et al. A systematic review on the applications of resting-state fMRI in Parkinson's disease: does dopamine replacement therapy play a role? *Cortex* 2015; **73**: 80–105. doi: https://doi.org/10.1016/j.cortex.2015.08.005
42. Badea L, Onu M, Wu T, Roceanu A, Bajenaru O. Exploring the reproducibility of functional connectivity alterations in Parkinson's disease. *Plos One* 2017; **12**: e0188196 doi: https://doi.org/10.1371/journal.pone.0188196
43. Chen Y, Storrs J, Tan L, Mazlack LJ, Lee J-H, Lu LJ, . Detecting brain structural changes as biomarker from magnetic resonance images using a local feature based SVM approach. *Journal of Neuroscience Methods* 2014; **221**: 22–31. doi: https://doi.org/10.1016/j.jneumeth.2013.09.001
44. Cuingnet R, Gerardin E, Tessieras J, Auzias G, Lehéricy S, Habert M-O, et al. Automatic classification of patients with Alzheimer's disease from structural MRI: a comparison of ten methods using the ADNI database. *NeuroImage* 2011; **56**: 766–81. doi: https://doi.org/10.1016/j.neuroimage.2010.06.013
45. Kloppel S, Stonnington CM, Chu C, Draganski B, Scahill RI, Rohrer JD, et al. Automatic classification of Mr scans in Alzheimer's disease. *Brain* 2008; **131**(Pt 3): 681–9. doi: https://doi.org/10.1093/brain/awm319